Nuclear Engineering and Technology 57 (2025) 103751

Contents lists available at ScienceDirect

Nuclear Engineering and Technology

journal homepage: www.elsevier.com/locate/net

Original Article

Uncertainty quantification of steady state depeltion solution using multi-physics coupling code system based on nodal diffusion code RAST-K

Jinsu Park [a], Yeongseok Kang [a], Deokjung Lee [a,b,*]

[a] Department of Nuclear Engineering, Ulsan National Institute of Science and Technology, UNIST-gil 50, Ulsan, 44919, Republic of Korea
[b] ANTS Co. Ltd., 406-21, Jongga-ro, Jung-gu, Ulsan, 44429, Republic of Korea

ARTICLE INFO

Keywords:
Multi-physics coupling framework
Nodal diffusion code RAST-K
Uncertainty quantification
Stochastic sampling
Nuclear data and input parameter perturbation

ABSTRACT

This study presents the uncertainty quantification results of steady-state depletion simulations using a multi-physics coupling framework based on the nodal diffusion code RAST-K. Developed for the analysis and optimization of pressurized water reactors, RAST-K integrates advanced methodologies and diverse engineering capabilities, consistently demonstrating strong agreement with measured data and commercial nuclear design codes. High-fidelity core simulations are conducted through the multi-physics coupling of RAST-K with the subchannel thermal-hydraulic code CTF and the fuel performance code FRAPCON. Notably, the consideration of dynamic gap conductance and thermal conductivity degradation in fuel performance calculations highlights discrepancies in pin-wise fuel temperature predictions. Uncertainty quantification is performed using stochastic sampling methods by perturbing both input parameters and nuclear data. The results indicate that uncertainties in global reactor design parameters, such as critical boron concentration, axial shape index, and peaking factor, are primarily driven by nuclear data perturbations, while thermal-hydraulic uncertainties are influenced by both input and nuclear data variations.

1. Introduction

Worldwide, reactor core analysis technology has been extensively developed, and each physics code in the nuclear research field is used independently. For example, power or heat flux data pre-generated from a neutronics code is used as input to simulate thermal-hydraulic (TH) or fuel performance calculations. This means that each physics code operates separately without complementary linkage. The one-way feedback coupling algorithm has the advantage of allowing easy use of each code system and obtaining conservative results. However, the demand for high-fidelity solutions that minimize conservatism has risen recently due to strengthened safety regulations. As a result, the development of multi-physics code systems has become a significant area of interest in nuclear research. In a one-way coupling system, conservatism accumulates because the conservative results from each standalone code are not reflected in subsequent calculations. In contrast, the two-way coupling method provides more accurate solutions by incorporating feedback between the results from each physics code.

A nodal diffusion code, RAST-K v2 [1], has been newly developed at the COmputational Reactor physics and Experiment (CORE) laboratory of the Ulsan National Institute of Science and Technology (UNIST) since 2014. RAST-K v2 is designed to achieve high accuracy and computational performance for pressurized water reactor (PWR) core analysis and design. It enables convenient core design, analysis, and coupling with other physics codes and platforms. RAST-K v2 has been validated using operational history data from functioning PWRs in South Korea [2]. Additionally, it is being used as a core simulator in machine learning applications with diverse objectives [3,4]. For convenience, RAST-K v2 is referred to simply as RAST-K throughout this paper.

Traditionally, pessimistic hypotheses are used in reactor safety analysis to ensure required safety margins. However, this approach often results in excessive conservatism. If safety regulations have been more enforced, the traditional approach may fail to satisfy safety margins. Therefore, reactor design and safety analysis typically include uncertainty quantification (UQ) and sensitivity analysis (SA) procedures to achieve accurate results along with confidence levels for best-estimate modeling and codes. In reactor analysis, various sources of uncertainty arise during computer code simulations. The most common sources are uncertainties from nuclear data (e.g., cross-sections) and input parameters (e.g., geometry and material properties for modeling). Two

* Corresponding author. Ulsan National Institute of Science and Technology, 50 UNIST-gil, Ulsan, 44919, Republic of Korea.
E-mail address: deokjung@unist.ac.kr (D. Lee).

https://doi.org/10.1016/j.net.2025.103751
Received 24 February 2025; Received in revised form 10 June 2025; Accepted 11 June 2025
Available online 13 June 2025
1738-5733/© 2025 Korean Nuclear Society, Published by Elsevier Korea LLC. This is an open access article under the CC BY-NC-ND license (http://creativecommons.org/licenses/by-nc-nd/4.0/).

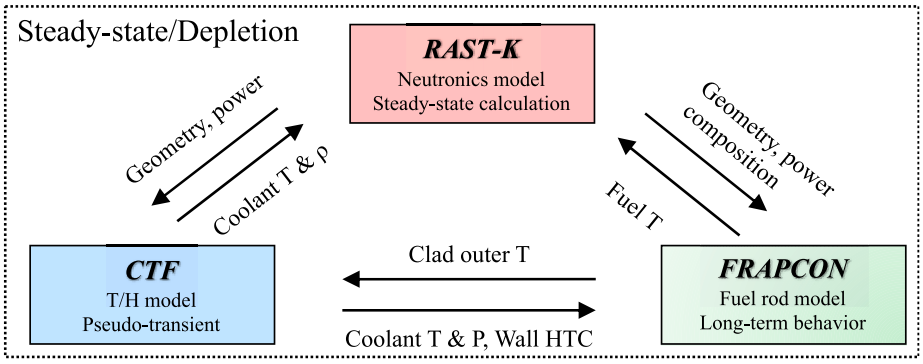

Fig. 1. Data exchange between the coupled codes.

primary methods are generally used for UQ. The deterministic method calculates system sensitivity to uncertain input parameters using perturbation theory (PT) and subsequently derives the covariance matrix. The second method, known as the stochastic sampling method, involves sampling uncertain input parameters provided in the Variance and Covariance Matrix (VCM) and performing statistical analysis on the resulting output responses. If nuclear data and input parameters are pre-generated according to their VCM, the stochastic sampling method can be easily employed for uncertainty quantification.

First, the multi-physics coupling scheme based on RAST-K is explained in Section 2. Second, Section 3 presents multi-cycle depletion calculation results obtained using the multi-physics code. Section 4 demonstrates the method for processing uncertainty sources from nuclear data and input parameters for stochastic sampling calculations. Finally, Section 5 provides a summary of the results.

2. Multi-physics couping method based on RAST-K

2.1. Summary of coupled codes

The simplified TH module is implemented in RAST-K [1] to update fuel and coolant temperatures by solving one-dimensional heat convection and transfer equations for a closed channel. The standalone TH module produces reliable results for steady-state conditions, such as reactor core design. For high-fidelity simulations, sub-channel TH codes and fuel performance codes are required for multi-physics coupling calculations. By coupling the sub-channel TH code, the two-fluid model is employed, which includes an expanded range of steam table properties and detailed heat transfer regimes at the cladding wall. Additionally, coupling with the fuel performance code allows for consideration of pellet-to-cladding interactions and detailed thermal conductivity information. The results from the coupled calculations, such as coolant and fuel temperatures, are directly used as feedback during neutronics calculations.

CTF (COBRA-TF) [5] is a TH simulation code designed for light water reactor (LWR) vessel analysis. For LWR modeling, CTF can solve sub-channel and 3D Cartesian forms of nine conservation equations. It uses a two-fluid modeling approach that accounts for three separate and independent flow fields (e.g., fluid film, vapor, and liquid droplets). Because CTF employs fine calculation units with detailed conservation equations for the flow field, it can perform multi-channel modeling with crossflow and obtain detailed coolant information. However, CTF utilizes a simplified heat structure model for fuel temperature calculations. Therefore, other physics codes, such as fuel performance codes, should be used for high-fidelity core analysis. CTF also supports parallel calculation capabilities through an assembly-wise domain decomposition technique.

FRAPCON [6] is a computer code that calculates the steady-state response of LWR fuel rods during long-term burnup. It evaluates fuel rod performance parameters such as temperature, pressure, and deformation based on the fuel rod power history and coolant boundary conditions. FRAPCON models various phenomena, including pellet-to-cladding heat transfer, mechanical deformation, pellet-to-cladding mechanical interaction, fission gas release, cladding oxidation, hydrogen pickup, pellet burnup, and power radial distribution.

The Fuel Rod Analysis Program Interface (FRAPI) [7,8] has been developed to effectively couple FRAPCON and FRAPTRAN with external codes. Both FRAPCON and FRAPTRAN are designed for single-pin fuel performance analysis. FRAPI provides features such as code initialization, time-step advancement, data exchange, saving and loading fuel rod data into computer memory or binary files, and writing restart files for FRAPTRAN. By independently allocating information for each fuel pin, FRAPI enables multi-rod simulations through iterative coupling schemes. Because each pin is modeled independently, FRAPCON and FRAPTRAN simulations can be easily parallelized.

Table 1
Summary of coupling parameters.

Variables	From	To	Unit
Fuel pin geometry	RAST-K	CTF/FRAPI	Pin to pin
Spacer grid information	RAST-K	CTF	–
Fuel composition (U-235 enrichment and gadolinia contents)	RAST-K	FRAPI	Pin to pin
Pin burnup	RAST-K	FRAPI	Pin to pin
Pin power	RAST-K	CTF/FRAPI	Pin to pin
Moderator direct heating fraction	RAST-K	CTF/FRAPI	–
Fuel radial temperature distribution	FRAPI	RAST-K	Pin to node
Cladding outer temperature	FRAPI	CTF	Pin to pin
Coolant temperature	CTF	RAST-K/ FRAPI	Pin to node/pin
Coolant density	CTF	RAST-K	Pin to node
Coolant pressure	CTF	FRAPI	Pin to pin
Coolant-to-cladding wall HTC	CTF	FRAPI	Pin to pin

2.2. Coupling parameters

The multi-physics code system based on RAST-K is established by coupling it with CTF and FRAPCON. Fig. 1 presents the data exchange diagram for multi-physics coupling during steady-state simulation. RAST-K handles neutronics simulations, calculating pin-wise power distribution based on given fuel and coolant conditions. As the main driver of the coupling system, RAST-K transfers core information, such as geometry and fuel rod composition, to CTF and FRAPI.

Using the core information from RAST-K, CTF initializes its

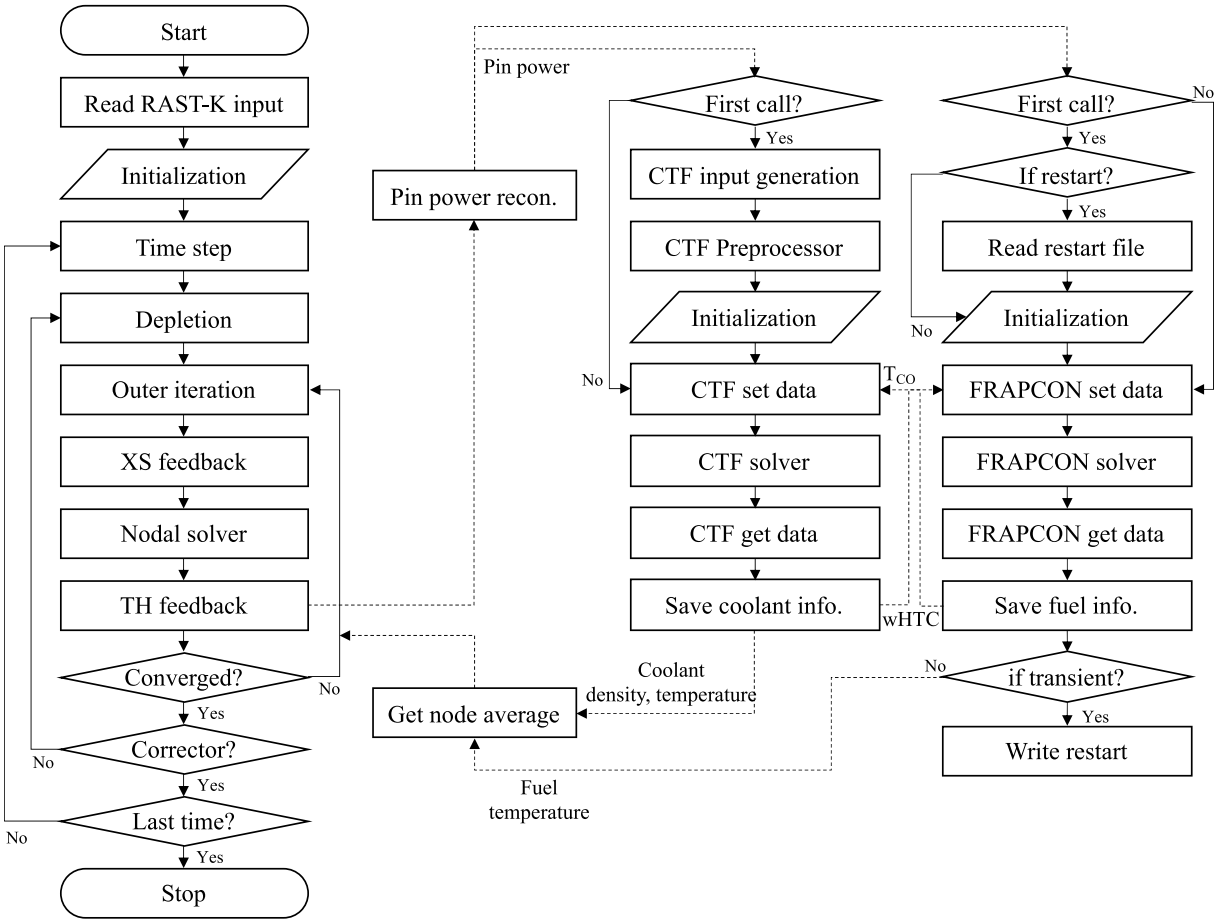

Fig. 2. Coupling algorithm for steady state calculation.

simulation. Pin-wise power and moderator direct heating fractions serve as heat flux sources for TH calculations. Since cladding outer surface temperatures are provided externally, CTF bypasses heat structure calculations. The pin-centered power distribution from RAST-K is directly transferred to CTF. Each pin, with four adjacent subchannels, receives an identical heat flux value for all four subchannels. CTF computes subchannel-level coolant temperatures, which are volume-averaged into pin-wise values.

Similarly, FRAPI initializes FRAPCON with fuel rod specifications from RAST-K, including geometry and fuel composition (e.g., U-235 enrichment and gadolinia content). To account for burnup and composition changes during sequential cycle depletion, FRAPI manages FRAPCON restart files. FRAPCON skips coolant heat convection calculations, using bulk coolant temperature and coolant-to-cladding heat transfer coefficients (HTC) as boundary conditions. It then calculates cladding outer surface temperatures, transferring them to CTF. Table 1 summarizes coupling parameters and their transfer directions.

2.3. Coupling algorithm

The RAST-K code serves as the central component of the coupling system, using the dynamic linked library (DLL) of CTF and the FRAPI source code to link with FRAPCON. CTF provides a coupling interface module containing essential subroutines. Fig. 2 illustrates the coupling algorithm for steady-state simulations in the multi-physics code system. At the start of each outer iteration step, it is important to provide physically reasonable TH conditions for accurate neutronics calculations. If spatially uniform temperatures (e.g., constant fuel and coolant temperature across the core) are used as initial guesses, the greater number of TH feedback is required for convergence of outer iteration. To address this, RAST-K employs an internal thermal feedback module that quickly provides node-wise and axially dependent temperature profiles. This approach stabilizes the neutronics solution from the beginning of outer iteration and reduces computational cost of subsequent CTF and FRAPCON calculations. Both codes are initialized during initialization phase of RAST-K. CTF initialization involves two steps: first, RAST-K generates four basic input files, which CTF preprocessing module converts into inputs based on the MPI calculation option. CTF is then initialized, establishing independent communication with RAST-K. Since CTF uses assembly-wise domain decomposition for MPI calculations, the number of processors must exceed the number of fuel assemblies. For FRAPCON, pin specifications are transferred via FRAPI, and restart files are loaded for cycle depletion calculations.

During outer iteration of RAST-K, TH information updates via calls to CTF and FRAPCON. If FRAPCON has not yet provided cladding temperatures in the first iteration, CTF uses its intrinsic heat structure model. CTF iteratively solves with its convergence criteria (e.g., mass and energy balance) and collects results from all MPI processes into the master process. RAST-K then saves pin-wise coolant information and converts it to node-wise values for cross-section feedback through volume weighting. Unlike CTF, FRAPCON includes fuel depletion modeling. Thus, RAST-K aligns its predictor-corrector steps with FRAPCON. During the corrector step, average pin power from both steps, along with coolant information and wall HTC, is used for fuel performance calculations. After gap pressure convergence, pin-wise fuel and cladding temperatures are stored in RAST-K and merged into node-wise distributions for cross-section feedback. Once the outer iteration converges, results are saved. CTF outputs are written via its intrinsic editing subroutine, and FRAPCON restart files are generated for subsequent cycle calculations.

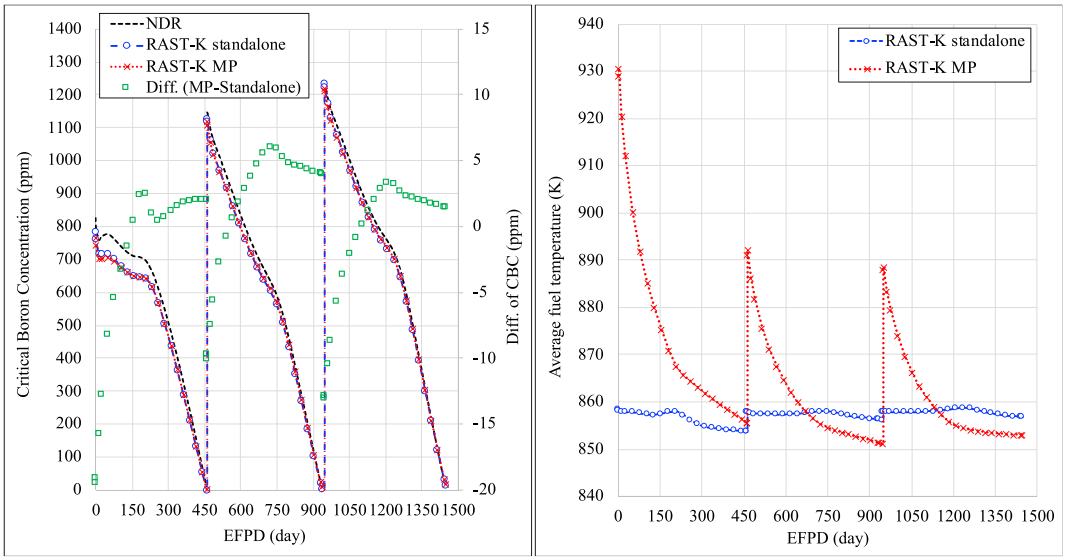

Fig. 3. CBC curve and core average fuel temperature behavior during three cycles of APR1400.

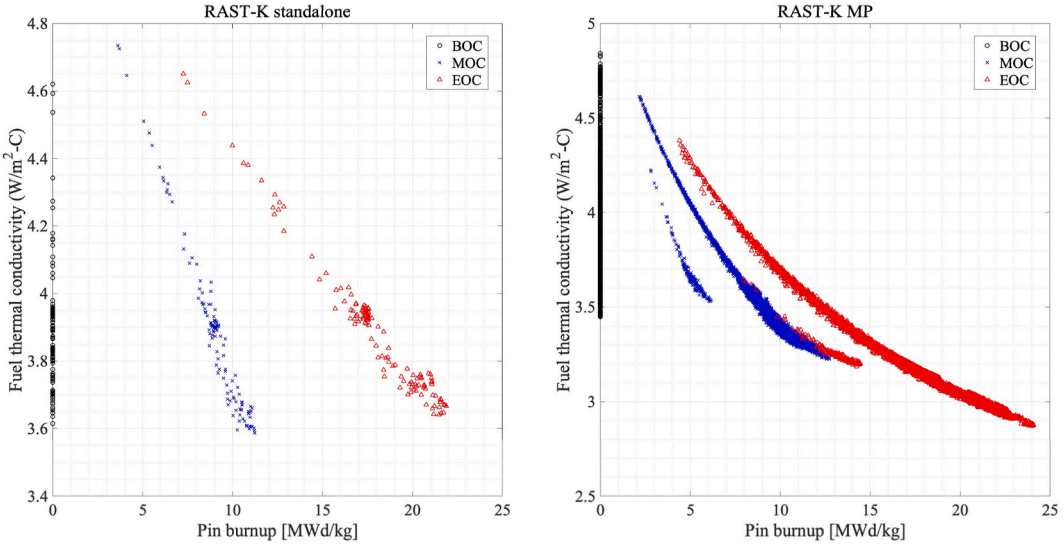

Fig. 4. Pin-wise fuel thermal conductivity along pin burnup.

3. Depletion calculation using multi-physics code

3.1. Multi-cycle depletion of APR1400 reactor core

RAST-K has been verified and validated using the operational history of Korean PWRs. A total of 114 cycles from 13 reactor cores, including OPR1000, APR1400, and Westinghouse type reactors were employed for core follow calculations [1,2]. The results were compared with commercial nuclear design code outputs and measurement data. To verify the multi-physics code system based on RAST-K, three depletion cycles (initial to third cycle) of the APR1400 [9] core were simulated. The RAST-K standalone simulation employed its internal TH solver without burnup-dependent thermal conductivity models, while the RAST-K MP simulation included CTF and FRAPCON for multi-physics coupling. The node-wise equivalent pin model is used for TH simulation. To see the effects of burnup dependent characteristics and subchannel-wise TH modeling, the multi-physics simulation with the CTF and FRAPCON is performed for the cycle depletion, and it is called by RAST-K MP in this paper.

3.2. Results from steady state depletion calculation

Fig. 3 shows the critical boron concentration (CBC) curve and core-average fuel temperature (Doppler temperature) for three APR1400 cycles. Fuel temperature increases due to thermal conductivity degradation (TCD) and ZrO_2 deposition, reducing reactivity with burnup. Despite TCD effects modeled in RAST-K MP, average fuel temperature is biggest at the beginning of each cycle and decreases with burnup due to dynamic gap conductance modeling. Although the fuel and cladding thermal conductivity decreases, the gap conductance gradually increases due to the decrement of size of gap between fuel and cladding by fuel swelling. The gap conductance is fixed as 10,000 W/m-K in the internal TH solver and the gap conductance of the fresh fuel is known as several thousand W/m-K. Therefore, the average fuel temperature of RAST-K MP is larger than that of RAST-K with internal TH solver at the beginning of each cycle. Therefore, the CBC of RAST-K MP is smaller than that of RAST-K standalone at initial cycle burnup of each cycle and the CBC of RAST-K MP increases after the middle of cycle.

Fig. 4 show the fuel thermal conductivity along burnup at BOC, MOC, and EOC of initial cycle using RAST-K standalone and RAST-K MP

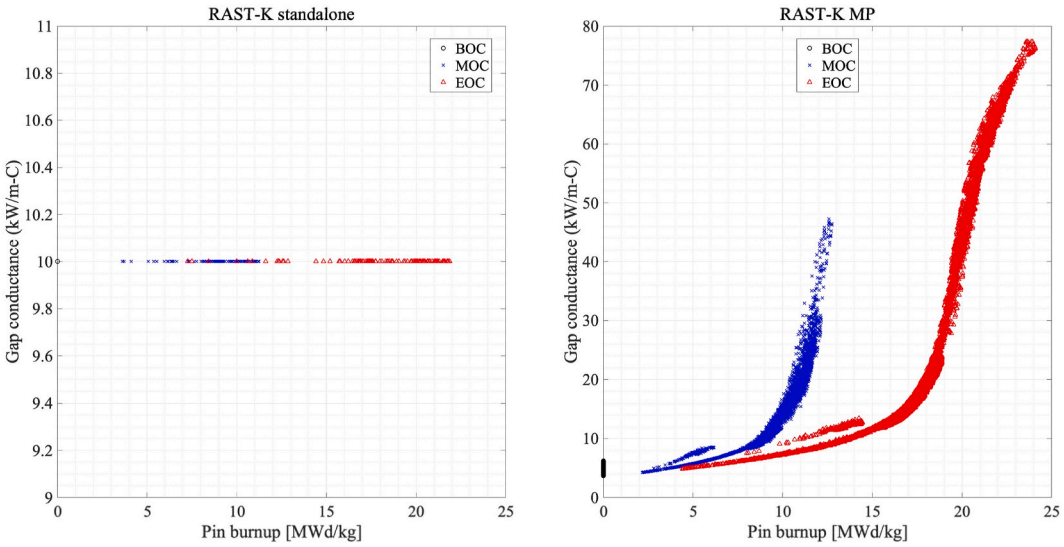

Fig. 5. Pin-wise gap conductance along pin burnup.

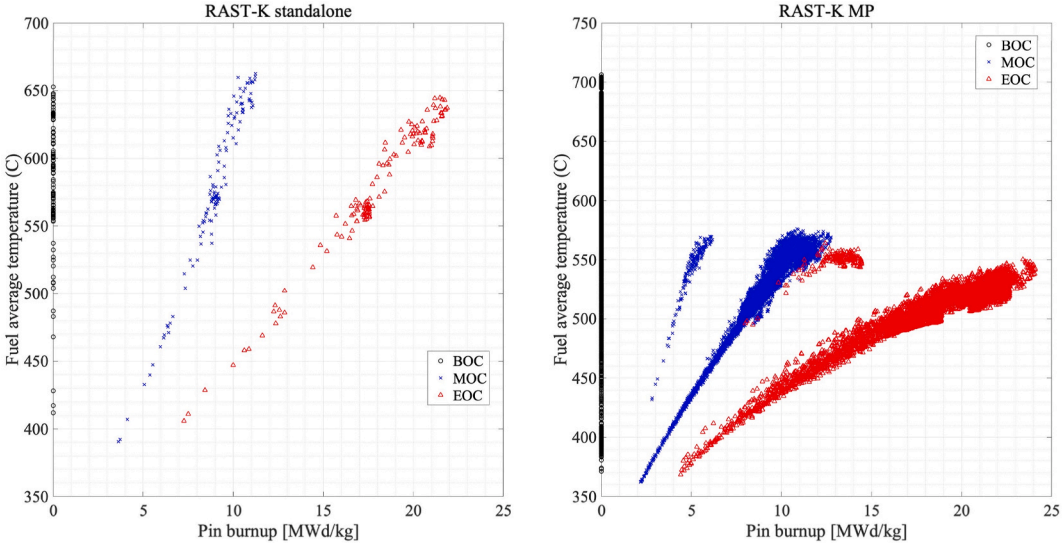

Fig. 6. Pin-wise average fuel temperature along pin burnup.

simulations. Because the RAST-K standalone calculation is performed with the node specification of the four-node per assembly, the thermal conductivity distribution is also expressed with four-node per assembly. As expected in forementioned section, the thermal conductivity degradation effect can be modeled in RAST-K MP. Because the smaller heat generated in the bigger burnup fuel, the thermal conductivity can be smaller by increasing fuel burnup in RAST-K standalone simulation. The thermal conductivity defects by considering fuel burnup in FRAPCON-4.0 NFI model can be captured in RAST-K MP simulation.

The gap conductance is fixed as 10 kW/m-C for internal TH solver of RAST-K standalone. However, the gap conductance is dynamically calculated based on fuel burnup and thermal-mechanical behavior in the RAST-K MP. Fig. 5 shows the variation of gap conductance versus fuel burnup at BOC, MOC, and EOC of initial cycle of APR1400. The gap conductance at BOC (corresponding to fresh fuel) is around 4–6 kW/m-C. At EOC, the gap conductance increases up to 80 kW/m-C due to the reduction of the fuel-cladding gap caused by fuel swelling and fuel-cladding mechanical interaction.

Fig. 6 shows pin-wise average fuel temperature versus fuel burnup. The RAST-K standalone simulation, using a fixed gap conductance, yields lower temperatures at BOC and higher at EOC. RAST-K MP, with dynamic gap conductance and TCD modeling, produces the opposite trend, indicating that gap conductance has a greater impact on fuel temperature than thermal conductivity.

Table 2
Summary of discrepancies of reactor design parameters from depletion calculation.

Parameter	RAST-K standalone	RAST-K MP
Critical boron concentration (ppm)	−29.47 ± 16.51	−30.38 ± 18.60
Axial shape index (−)	0.0081 ± 0.0103	0.0078 ± 0.0098
Normalized FA power (−)	0.001 ± 0.013	0.001 ± 0.015

The CBC discrepancy with NDR results ranges from −70 to 10 ppm for both simulations. Table 2 summarizes depletion calculation results, including CBC, axial shape index (ASI), and normalized fuel assembly (FA) power. Both RAST-K standalone and MP results show reasonable agreement with the NDR data, with deviations generally within ±50 ppm in CBC, which is considered acceptable for code verification. Although the specific code used in the NDR is confidential and cannot be

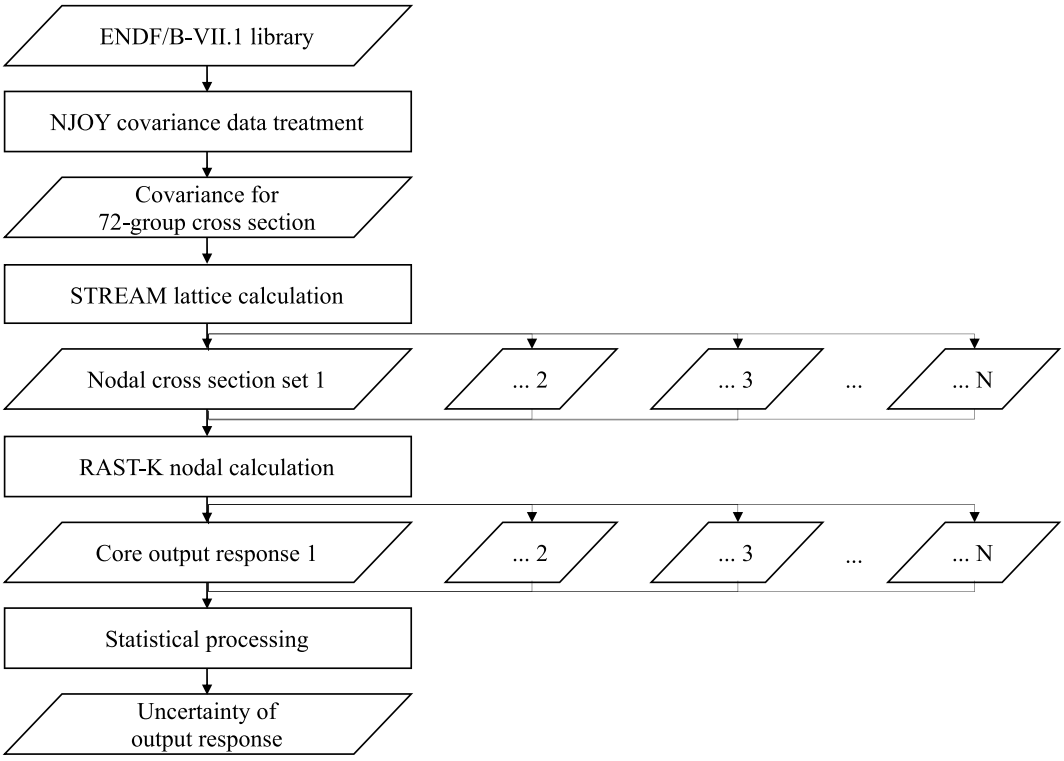

Fig. 7. Flowchart of uncertainty propagation for nuclear data.

disclosed, previous studies [1] confirms that both NDR and RAST-K simulation results align with measured CBC value within ±50 ppm.

4. Uncertainty quantification using multi-physics code

4.1. Stochastic sampling method

Several studies have addressed uncertainty propagation in reactor core modeling and simulation using various UQ methodologies. Common approaches include deterministic and stochastic sampling methods to propagate input uncertainty to output responses. In deterministic methods, sensitivity coefficients and input parameter covariance matrices are calculated based on first-order perturbation theory (PT). Output uncertainties are then derived using the Sandwich rule from sensitivities and the variance-covariance matrix (VCM). Conversely, stochastic methods employ random sampling of input parameters, enabling statistical analysis of perturbed output responses. Variance is computed using Eq. (1).

$$\mathrm{Var}[R] = \frac{\sum_{i=1}^{N_s}(R_i - \overline{R})^2}{N_s - 1}, \tag{1}$$

where N_s is the number of samples and $\overline{R}$ is the mean of the response. From the repeated N_s calculations, the resulting output responses can be analyzed with standard statistical analysis by assuming that the probability density function (PDF) of the responses is a normal distribution. The uncertainty of σ_p in an individual output response can be calculated by taking the square root of the variance in Eq. (1).

For the various output responses including reactor design parameters from multi-cycle depletion simulations, the normality test should be performed to verify this normality assumption. In this research, the Shapiro-Wilk test is employed for the normality test [10]. The Shapiro-Wilk test tests the null hypothesis that a sample came from a normally distributed population. If the p-value falls below a significant level of 5 %, the null hypothesis is rejected, and the sample distribution is not following the normal distribution. If the normality assumption is accepted, the confidence bounds of uncertainties of output responses can be computed. For the true mean μ and true standard deviation σ_{true}, the constructed parameter χ^2 can be computed as Eq. (2).

$$\chi^2 = \frac{(N_s - 1)\sigma_p^2}{\sigma_{true}^2}, \tag{2}$$

The σ_p^2 is the sample variance and the parameter χ^2 follows the chi-distribution with $N_s - 1$ degree of freedom. For a one-sided and two-sided uncertainty parameter, the criteria of 95 % confidence level indicates that 95 % of the χ^2 value is bounded inside the interval of $\left[\chi^2_{1-\alpha}, \infty\right]$ and $\left[\chi^2_{1-\alpha/2}, \chi^2_{\alpha/2}\right]$ each. Then, the confidence interval of the standard deviation is derived as Eq. (3) and Eq. (4) for one-sided upper and two-sided bounds.

$$\frac{(N_s - 1)\sigma_p^2}{\chi^2_{\alpha/2}} < \sigma_{true}^2 < \frac{(N_s - 1)\sigma_p^2}{\chi^2_{1-\alpha/2}}, \tag{3}$$

$$\sigma_{true}^2 < \frac{(N_s - 1)\sigma_p^2}{\chi^2_{1-\alpha}}, \tag{4}$$

Stochastic sampling typically requires numerous simulations, which is computationally expensive. To mitigate this, Latin hypercube sampling (LHS) is employed to generate controlled random samples by partitioning the cumulative density function into even regions and selecting one random point per region.

4.1.1. Nuclear data perturbation

For uncertainty propagation from nuclear data, the stochastic sampling method is applied to transport lattice calculations. Fig. 7 shows the flowchart of uncertainty propagation from nuclear data to uncertainty of core output response. The nuclear data uncertainty is propagated through the lattice calculation to the two-group nodal cross section used in RAST-K. Since the group constant is generated by the lattice code STREAM [11,12], the perturbed cross section files should be pre-generated before nodal calculation. In this research, covariance for

Table 3
Information of input parameters for uncertainty quantification.

Parameter	Code			Uncertainty		Dist.
	N	T	F	Relative	Absolute	
Core power (MW)	O	O	O	1.0 %		Normal
Coolant flow rate (kg/s)		O		1.5 %		Normal
System pressure (bar)		O		1.0 %		Normal
Inlet temperature (C)		O		1.0 %		Normal
Turbulent-mixing coefficient (−)		O		5.0 %		Uniform
Weighting factor for void drift model (−)		O		5.0 %		Uniform
Pellet density (%TD)			O		0.3033	Normal
Pellet outer diameter (cm)		O	O		0.0082	Uniform
Initial gap thickness (cm)		O	O		0.0004	Uniform
Cladding thickness (cm)		O	O		0.0005	Uniform
Rod fill gas pressure (MPa)			O		0.0233	Normal
Plenum length			O		0.3800	Normal
U-235 concentration (w/o)			O		0.0007	Normal
Gadolinia enrichment (wt.%)			O		0.1086	Normal
Pellet roughness (micron)			O		0.1667	Normal
Cladding roughness (micron)			O		0.1000	Normal
Space grid width (cm)		O		1.0 %		Normal
Spacer grid loss coefficient (−)		O		1.0 %		Normal
Guide tube inner diameter (cm)		O		1.0 %		Normal
Guide tuber outer diameter (cm)		O		1.0 %		Normal
Dish shoulder width (cm)			O	1.0 %		Normal
Dish height (cm)			O	1.0 %		Normal
Gamma fraction (−)		O	O	1.0 %		Normal

scattering, fission, capture, fission spectrum, and number of neutrons per fission are considered by following the method invented by A. Yamamoto [13]. The 72-group covariance matrix for 144 nuclides is generated by using the NJOY-99 [14] based on ENDF/B-VII.1 library. Based on this procedure, total 500 sets of perturbed nodal cross section are pre-generated. To simulate the three cycles of APR1400, total 37 nodal cross section sets are generated including 32 fuel assembly models and 5 reflector assembly models.

4.1.2. Input parameter perturbation

Since the multi-physics code is used to simulate a high-fidelity model rather simplified (lumped) model, the detailed technological and operational data are required as an input data. By considering the uncertainty from input data such as manufacturing, geometry, boundary conditions, and core conditions, the impact of input parameter uncertainty propagation on output response can be quantified. In previous work about uncertainty propagation from input data, the uncertainty propagation of the Doppler temperature is utilized instead of uncertainty from the material property such as thermal conductivity of fuel and cladding [15]. However, the uncertainties from fuel manufacturing and modeling are directly considered in this research.

Table 3 represents the information of input parameters to be used for uncertainty quantification using multi-physics code. Each parameter is used as an input of each physics code. In Table 3, "N", "T", and "F" represent each physics code (N: Neutronics code; T: Thermal-hydraulic code, F: Fuel performance code). For example, the core power is used for every physics part, and the coolant flow rate is used for only thermal-hydraulic part. The input parameters of CTF include boundary conditions such as inlet temperature and system pressure, geometry to model the subchannel and spacer grid, and factor to model physical phenomenon. The detail information for modeling the geometry and composition of fuel pellet is used in FRAPCON. The uncertainty of each input parameter is referred from the previous work done by expert of each physics [16,17]. If there is no information of uncertainty, 1.0 % relative standard deviation with normal distribution is used for input perturbation. The input parameter perturbation is performed on the fly during calculation based on Latin hypercube sampling method.

4.2. Uncertainty quantification of reactor design parameters

The uncertainties in reactor design parameters are quantified using the stochastic sampling method with RAST-K. More than 124 depletion calculations are performed for both RAST-K standalone and RAST-K MP, simulating three APR1400 cycles. Key reactor design parameters such as CBC, ASI, and maximum fuel centerline temperature, are selected as core output responses. In total, 500 simulations are performed for RAST-K standalone, while 124 simulations are run for RAST-K MP due to higher computational cost.

Fig. 8 presents the evolution and statistical analysis of critical boron concentration (CBC) over three cycles for both RAST-K standalone and RAST-K MP. The nominal value, median, sample mean, and standard deviation are displayed, with 95 % confidence intervals shown in red and green. Discrepancies between sample mean and nominal CBC are under 10 ppm, indicating no bias from nuclear data and input parameter perturbations. The Shapiro-Wilk normality test results (p-values >0.05) support the normality assumption. The true standard deviation from RAST-K standalone is bounded by [94.2 %σ_p, 106.6 %σ_p] at 95 % confidence, while for RAST-K MP, it is [88.9 %σ_p, 114.3 %σ_p], reflecting the smaller sample size. CBC uncertainty decreases with fuel burnup per

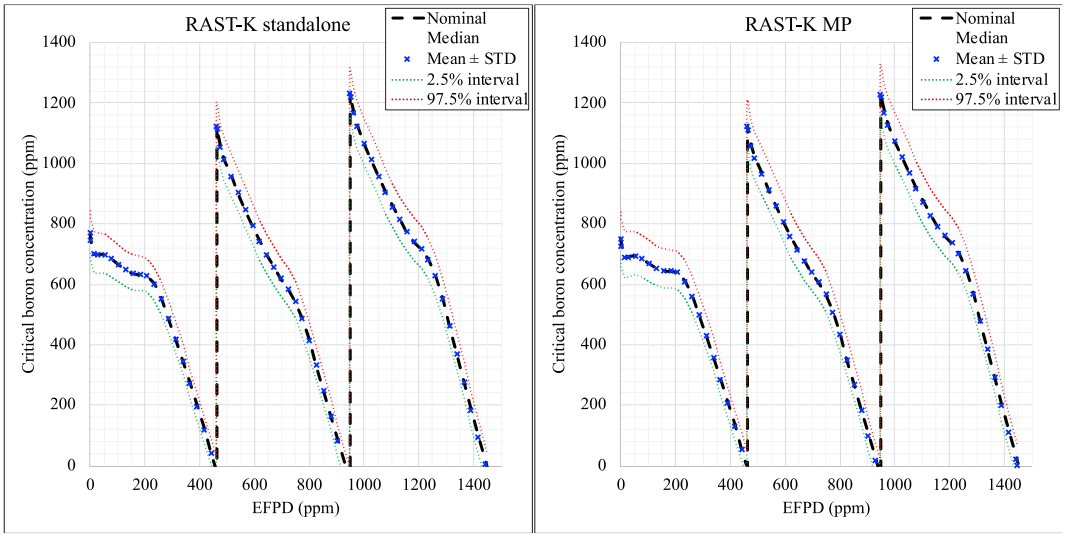

Fig. 8. Evolution of CBC of APR1400 and its statistics using RAST-K standalone and RAST-K MP.

Table 4
Statistics of pin peaking factor at BOC, MOC, and EOC during multi cycles using RAST-K standalone and RAST-K MP.

Cycle	State	RAST-K Standalone		RAST-K MP	
		Nominal	Mean ± STD	Nominal	Mean ± STD
1st	BOC	1.9196	1.9375 ± 0.0191	1.9213	1.9449 ± 0.0210
	MOC	1.7079	1.7111 ± 0.0131	1.7172	1.7202 ± 0.0140
	EOC	1.6146	1.6164 ± 0.0310	1.6194	1.6234 ± 0.0306
2nd	BOC	1.7491	1.7520 ± 0.0167	1.7656	1.7647 ± 0.0158
	MOC	1.6877	1.6944 ± 0.0090	1.6988	1.7063 ± 0.0122
	EOC	1.6534	1.6670 ± 0.0408	1.6730	1.6863 ± 0.0363
3rd	BOC	1.5990	1.6134 ± 0.0201	1.6138	1.6245 ± 0.0206
	MOC	1.6629	1.6756 ± 0.0173	1.6833	1.6964 ± 0.0183
	EOC	1.5937	1.6041 ± 0.0383	1.6118	1.6220 ± 0.0326

cycle, though RAST-K MP shows relatively higher uncertainty.

Table 4 details the statistical results for 3D pin power peaking factor (Fq) at BOC, MOC, and EOC across three cycles. Minimal discrepancies between nominal and mean values confirm unbiased sampling. The true standard deviation bounds are [0, 106.6 %σ_p] for 500 samples and [0, 111.8 %σ_p] for 124 samples at 95 % confidence. For burnup steps with non-normal Fq distributions, the 95th percentile is used. Slightly larger Fq uncertainty is observed at EOC.

Fig. 9 shows assembly power distributions and uncertainties at BOC, MOC, and EOC of the third cycle. Nominal, sample mean, and standard deviation values are presented. Peripheral assembly power uncertainties exceed those of central assemblies, with negligible differences between RAST-K standalone and RAST-K MP results.

Fig. 10 illustrates axial power shapes and uncertainties at BOC, MOC, and EOC of the third cycle. Discrepancies between RAST-K standalone

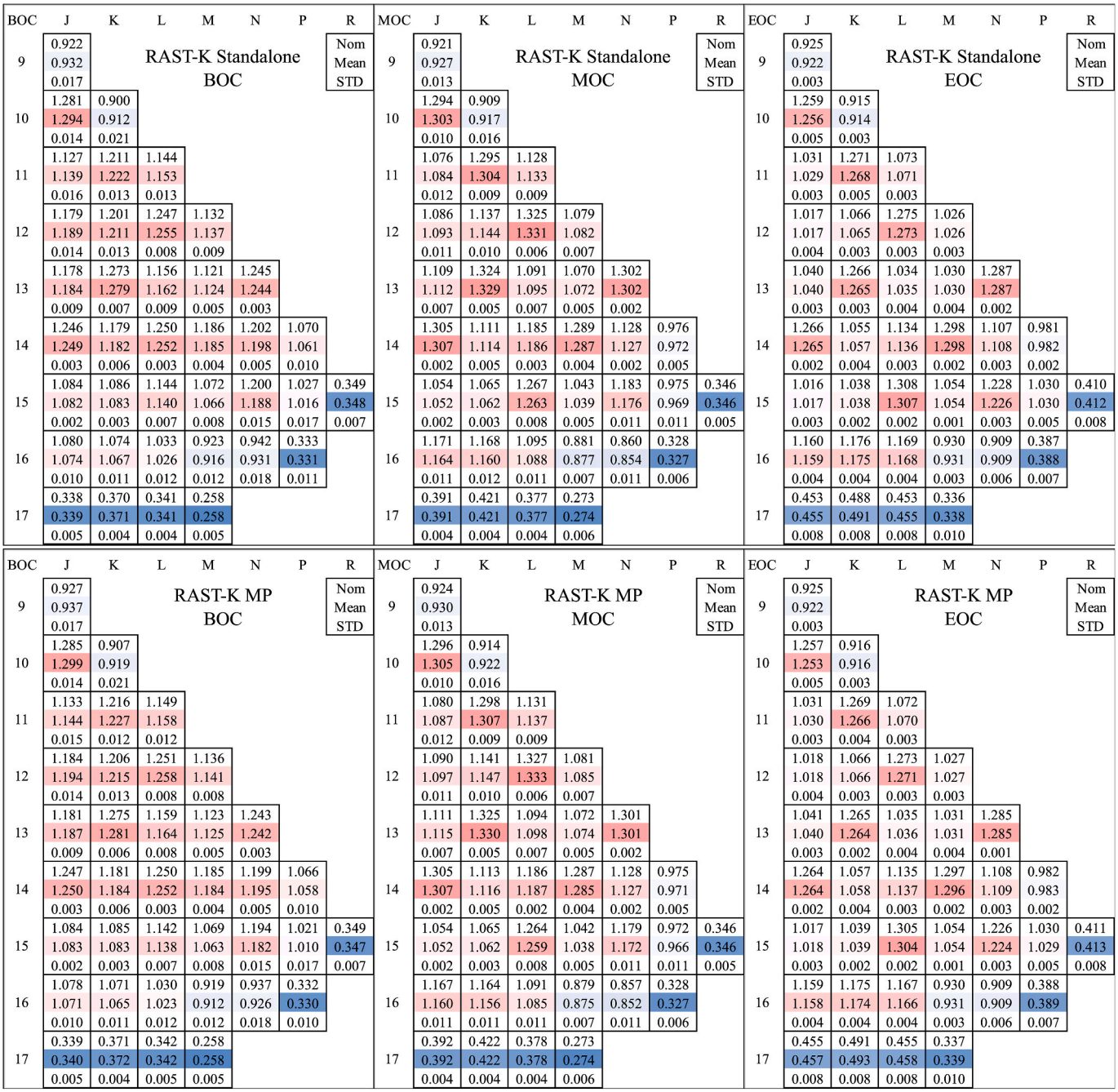

Fig. 9. Assembly power distribution and its uncertainty at BOC, MOC, and EOC for 3rd cycle using RAST-K standalone and RAST-K MP.

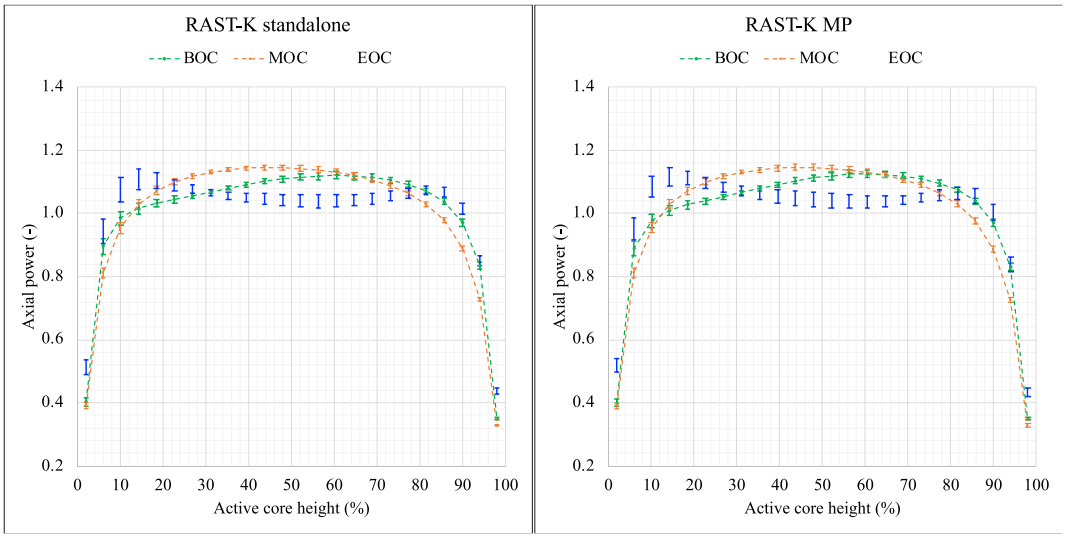

Fig. 10. Axial power shape and its uncertainty at BOC, MOC, and EOC for 3rd cycle using RAST-K standalone and RAST-K MP.

Table 5
Summary of uncertainty quantification on selected core output responses from 3rd cycle depletion calculation.

Parameter	State	All	Input parameter	Nuclear Data
Critical boron concentration (ppm)	BOC	1231.91 ± 79.77	1232.72 ± 2.47	1232.07 ± 80.00
	MOC	743.58 ± 69.46	741.86 ± 4.08	743.64 ± 69.63
	EOC	−10.97 ± 54.39	−6.06 ± 7.79	−10.60 ± 53.76
Axial shape index (−)	BOC	−0.0071 ± 0.0076	−0.0083 ± 0.0004	−0.0073 ± 0.0066
	MOC	0.0181 ± 0.0067	0.0181 ± 0.0022	0.0179 ± 0.0046
	EOC	0.0166 ± 0.0127	0.0158 ± 0.0048	0.0167 ± 0.0118
Peaking factor (−)	BOC	1.6134 ± 0.0201	1.6011 ± 0.0027	1.6124 ± 0.0212
	MOC	1.6756 ± 0.0173	1.6629 ± 0.0055	1.6748 ± 0.0171
	EOC	1.6041 ± 0.0383	1.5938 ± 0.0148	1.6021 ± 0.0343
Maximum fuel centerline temperature (C)	BOC	1262.01 ± 21.94	1256.64 ± 14.66	1261.97 ± 14.43
	MOC	1349.24 ± 23.31	1337.54 ± 16.69	1348.76 ± 16.54
	EOC	1399.38 ± 29.25	1388.52 ± 19.94	1395.24 ± 24.28

and RAST-K MP results are minor. Average uncertainties in axial power shape are 1.10 %, 0.93 %, and 2.08 %, increasing with fuel burnup.

Table 5 summarizes core output responses and uncertainties from the third cycle depletion calculation. Input parameter and nuclear data perturbations are analyzed separately. For CBC, ASI, and Fq, nuclear data perturbation contributes significantly more to uncertainty than input parameter perturbation. Input parameters have minimal impact on global parameters such as CBC and ASI. The relative standard deviation of maximum fuel centerline temperature by perturbing both input parameter and nuclear data is around 1.7–2.1 %. The uncertainties of maximum fuel centerline temperature coming from each perturbation are similar level of 1.1–1.8 % for all core states. The result from TH feedback calculation like fuel centerline temperature is directly affected by the perturbation of input parameter. Therefore, the perturbations of input parameter and nuclear data contribute similar level of uncertainty on core response, which directly related with TH feedback calculation.

5. Conclusion

In this paper, the uncertainty quantification results for steady-state depletion simulations are presented using a multi-physics coupling code based on the RAST-K nodal diffusion code. RAST-K, developed for PWR design and analysis, employs advanced methodologies and engineering features, demonstrating strong agreement with both measured data and commercial nuclear design codes.

High-fidelity core simulations are achieved through multi-physics coupling with the CTF subchannel TH code and the FRAPCON fuel performance code. Geometry and pin-wise heat generation data from the neutronics code are passed to the TH and fuel performance codes, while temperature outputs from these codes provide cross-section feedback to the neutronics module. Multi-cycle depletion calculations are performed using this integrated system.

The current assumptions for TH calculations effectively ensure high accuracy under steady-state conditions, resulting in minimal discrepancies in reactor design parameters. However, pin-wise fuel temperatures differ due to dynamic gap conductance and TCD effects modeled in the fuel performance code.

Uncertainty quantification is conducted using stochastic sampling, with perturbations applied to both input parameters and nuclear data. The UQ results for RAST-K standalone and MP calculations show similar reactor design parameters and uncertainty levels. Analysis of uncertainty contributions indicates that nuclear data perturbations predominantly affect global design parameters, such as CBC, ASI, and the power peaking factor. In contrast, TH related parameters, such as maximum fuel centerline temperature, are influenced by perturbations in both input parameters and nuclear data.

CRediT authorship contribution statement

Jinsu Park: Writing – original draft, Methodology, Conceptualization. **Yeongseok Kang:** Writing – review & editing. **Deokjung Lee:** Supervision.

Declaration of competing interest

The authors declare that they have no known competing financial

interests or personal relationships that could have appeared to influence the work reported in this paper.

Acknowledgements

This work was supported by the Innovative Small Modular Reactor Development Agency grant funded by the Korea Government (RS-2023-00265742).

References

[1] J. Park, J. Jang, H. Kim, J. Choe, D. Yun, P. Zhang, A. Cherezov, D. Lee, RAST-K v2 - three-dimensional nodal diffusion code for pressurized water reactor core analysis, Energies 13 (2020), https://doi.org/10.3390/en13236324.
[2] J. Choe, S. Choi, P. Zhang, J. Park, W. Kim, H. Shin, H. Lee, D.J. Jung, D. Lee, Verification and validation of STREAM/RAST-K for PWR analysis, Nucl. Eng. Technol. 51 (2019) 356–368, https://doi.org/10.1016/j.net.2018.10.004.
[3] H. Kim, Y. Jo, D. Lee, Feasibility study of AI-based prediction for CRUD induced power shift in PWR, In Proceedings of the KNS Autumn Meeting Korea 2021. Oct 20-22.
[4] S. Dzianisau, K. Saeju, H. Lee, D. Lee, Development of an artificial neural network model for generating macroscopic cross-sections for RAST-AI, Ann. Nucl. Energy 186 (2023), https://doi.org/10.1016/j.anucene.2023.109777.
[5] COBRA-TF Subchannel Thermal-Hydraulics Code (CTF), Theory Manual Revision 0, Pennsylvania State University, 2015. Technical Report No. CASL-U-2015-0054-000.
[6] FRAPCON-4, 0: a Computer Code for the Calculation of Steady-State, Thermal-Mechanical Behavior of Oxide Fuel Rods for High Burnup, Pacific Northwest National Laboratory, 2018. Technical Report No. PNNL-19418.
[7] A. Cherezov, J. Park, H. Kim, J. Choe, D. Lee, MPCORE multiphysics system for light-water reactor core safety analysis and accident simulation, Energies 13 (2020), https://doi.org/10.3390/en13236374.
[8] A. Cherezov, J. Park, H. Kim, D. Lee, MPCORE code for OPR-1000 transient multi-physics simulation with adaptive time step size control, In Proceedings of the ANS Summer Meeting USA 2020. Jun 8–11.
[9] APR1400 Reactor Core Benchmark Problem Book, Korea Atomic Energy Research Institute, 2019. Technical Report No. RPL-INERI- CA-004.
[10] B.W. Yap, C.H. Sim, Comparisons of various types of normality tests, J. Stat. Comput. Simulat. 81 (2011) 2141–2155, https://doi.org/10.1080/00949655.2010.520163.
[11] S. Choi, C. Lee, D. Lee, Resonance treatment using pin-based pointwise energy slowing-down method, J. Comput. Phys. 330 (2017) 134–155, https://doi.org/10.1016/j.jcp.2016.11.007.
[12] S. Choi, D. Lee, Three-dimensional method of Characteristics/diamond-difference transport analysis method in STREAM for whole-core neutron transport calculation, Comput. Phys. Commun. 260 (2021), https://doi.org/10.1016/j.cpc.2020.107332.
[13] A. Yamamoto, K. Kinoshita, T. Watanabe, T. Endo, Uncertainty quantification of LWR core characteristics using random sampling method, Nucl. Sci. Eng. 181 (2015) 160–174, https://doi.org/10.13182/NSE14-152.
[14] R. Arcilla, A.C. Kahler, P. Oblozinsky, M. Herman, Processing neutron cross section covariances using NJOY-99 and PUFF-IV, Nucl. Data Sheets 109 (2008) 2910–2914, https://doi.org/10.1016/j.nds.2008.11.033.
[15] J. Hou, M. Avramova, K. Ivanov, Best-estimate plus uncertainty framework for multiscale, multiphysics light water reactor core analysis, Sci. Technol. Nucl. Instal. 2020 (2020) 18, https://doi.org/10.1155/2020/7526864.
[16] K. Borowiec, T. Kozlowski, C.S. Brooks, Validation and uncertainty quantification for two-phase natural circulation flows using TRACE code, Nucl. Sci. Eng. 194 (2020) 737–747, https://doi.org/10.1080/00295639.2020.1713671.
[17] Evaluation of ECCS Performance of Kori Unit 1 Using KINS Best-Estimate Methodology, Korea Institute of Nuclear Safety KINS/RR-531 (2007).